Nigerian Journal of Technology (NIJOTECH)
Vol. 43, No. 2, June, 2024, pp.353 - 363
www.nijotech.com

Print ISSN: 0331-8443
Electronic ISSN: 2467-8821
https://doi.org/10.4314/njt.v43i2.19

MICROCONTROLLER-BASED FACTS DEVICES IMPLEMENTATION

AUTHORS:
V. C. Madueme[1,*], A. O. Ekwue[2], E. C. Ejiogu[3], and V. O. Ajah[4]

AFFILIATIONS:
[1,2,3]Department of Electrical Engineering, University of Nigeria Nsukka, Nigeria.
[2,3,4]Africa Centre of Excellence for Sustainable Power and Energy Development, University of Nigeria Nsukka, Nigeria.

***CORRESPONDING AUTHOR:**
Email: victory.madueme@unn.edu.ng

ARTICLE HISTORY:
Received: 12 April, 2023.
Revised: 26 October, 2023.
Accepted: 26 March, 2024.
Published: 12 June, 2024.

KEYWORDS:
FACTS, Load displacement, Power factor, Reactive power, SVC, Voltage.

ARTICLE INCLUDES:
Peer review

DATA AVAILABILITY:
On request from author(s)

EDITORS:
Patrick Udemeobong Akpan

FUNDING:
None

Abstract

In power systems, the case of voltage control, power factor improvement and reactive power management cannot be over-emphasized. In developing countries such as Nigeria, the electricity power system is characterized by operational constraints which are predominantly poor power quality, voltage fluctuations and increased power losses among others. Furthermore, these frequent system disturbances contribute to the unreliability of such power system. This paper looks at the thyristor-switched capacitor- thyristor-controlled reactor (TSC-TCR), static volt-ampere-reactive controller (SVC), a flexible alternating current transmission system (FACTS) device as a solution to mitigate the thermal and voltage problems associated with the Nigerian network. A microcontroller-based SVC prototype was designed in Proteus software and implemented in a laboratory environment using locally available discrete electronic components for load power factor correction based on distributed reactive power control. The microcontroller was in charge of carrying out the logic control scheme for the two branches and computing the load displacement power factor (PFD). The SVC was found to improve the PFD by 44.78% under inductive loading where the power factor increased significantly from 0.67 to 0.97.

1.0 INTRODUCTION

The rise in population has led to an increased gap between power demand and supply in many countries [1]. As the power demand continues to increase rapidly across the globe, due to the ever-growing population and economic growth, electrical power systems face new and complex challenges. There is no question that a sizable portion of the challenges facing the energy and power sector are related to maintaining, controlling, and supervising both voltage control and reactive power (Q measured in Mega-Var) [2]. As a result, power shortages that differ significantly between generated power and load demand are alarming [3]. In developing countries, these challenges include attaining a controllable, reliable, and secure system that operates within certain standard limits giving the dynamic, complex, and nonlinear nature of electric power systems [4]. Technically speaking, one of the key causes of inadequate power supply is increased transmission line active power losses [5]. Harmonics may also lead to malfunctioning of power system components [6].

Voltage instability has been a major contributing factor to recent complete or partial system failures in

HOW TO CITE:
Madueme, V. C., Ekwue, A. O., Ejiogu, E. C., and Ajah, V. O. "Microcontroller-Based Facts Devices Implementation", *Nigerian Journal of Technology*, 2024; 43(2), pp. 353 – 363; *https://doi.org/10.4314/njt.v43i2.19*

the Nigerian power system [7]. According to [8], Nigerian power grid is generally weak and characterized by a highly unreliable energy supply. Though, the network can transmit about 6050 MW, it is very sensitive to major disturbances [9], [10]. In [11], the study showed that the Nigeria national grid performed abysmally in meeting the electricity demand of the populace and according to [12], there are technical obstacles to the interconnection's stability because of the configuration of the Nigerian interconnected system, which consists of long power lines and few generators. There are difficulties with Nigeria's transmission network because of the country's topography and a 20,000 km long transmission line [13]. Hence, The need to maintain grid stability and the rising demand for electricity make protecting these transmission lines essential [14]. However, in order to successfully and efficiently transmit electricity to every part of the country, the efficiency of Nigeria's 330kV transmission network needs to be increased [15].

As a result, it becomes highly imperative to control the power flow along the transmission corridor [16]. According to [17] in their study of voltage stability in Nigeria, pointed out that the problems as stated in [10], [11] are due to unplanned electrical energy demand as well as the use of obsolete transmission network. The demand for electric power is too high than the supply and the Nigerian state seems not to be able to install new transmission facilities to mitigate the shortage [18]. It is clear that the current state of power generation in Nigeria poses a challenge to our capacity to reevaluate the delivery of energy at the highest possible efficiency [19]. As a result, in order to add more energy resources and achieve more growing load connectivity in the current electrical power network, it is necessary to continuously review the topology, components, and dynamics of the power system [20].

To determine and solve the many problems of the power system network, there is need to regulate the system stability [21]. Hence, power system analysis is essential such as the creation of a system load flow model [22]. This entails running simulations and calculations to confirm that the electrical system, along with its component parts, are appropriately specified to function as intended, withstand anticipated stress, and be safeguarded against malfunctions. After carrying out power system analysis to determine possible problems associated with the power system network comes the task of determining the best and fast means of solving the problems [23]. Thankfully, advancement in technology and standards focused on the improvement of the grid and the power systems have provided us with technologies that allow us to utilize existing power systems. One of these technologies is the Flexible Alternating Current Transmission System (FACTS) such as the Static Volt-Ampere-Reactive Compensator (SVC).

Several studies and trials have been documented in literature regarding the use and effectiveness of SVC on the power system network. A survey by [24] investigated that the SVC could be used to improve the stability of a transmission network. FACTS technologies allow for improved transmission system operation compared to the construction of new transmission lines [25]. Through stability enhancement, FACTS devices have demonstrated excellent power transfer capabilities by restoring the voltage magnitude profiles at the buses that had previously experienced voltage dips [26]. The goal of this paper is to study or investigate the effect of increase in dynamic power factor and balance the source side currents whenever necessary.

FACTS devices are basically obtained from foreign companies by the Nigerian power Industry. Unfortunately, they are very costly and with the depreciation of the Nigerian currency, it is fast becoming out of reach for procurement by the Nigerian power Industry. In addition, it is a known fact that distortions exist in the ratings of FACTS devices produced by various companies which affects efficiency at the implementation stage. Hence, this behoves the need to find cheaper alternatives with standardized ratings to suit the needs of the Nigerian power industry. It is upon this premise that this research was done using locally available materials in the country with standardized ratings for the prototype. Its efficiency with respect to power factor control was also established in the prototype.

Authors such as [23-25] who worked on the Nigerian power system focused only on simulation application of FACTS. However, this work went further to implement a distributed SVC prototype that optimizes power factor in real time. This is a work implemented in Nigeria with locally available materials which have cheaper cost implications. This is important for commercialization and has positive implications for developing research and development (R&D) industries and reduction of youth unemployment in the Nigerian power sector.

2.0 METHODOLOGY

2.1 Reactive Power Control of the TSC-TCR SVC Scheme

Generally, the total VAR output for the TSC-TCR SVC circuit is:

$$Q = V[I_{LF}(\alpha) - \sum I_{Cn}] \quad (1)$$

Where, Q is the total SVC VAR output, V is the supply voltage, $I_{LF}(\alpha)$ is the inductive current absorbed by the inductor (TCR), $\sum I_{Cn}$ is the total injected current drawn by the capacitor (TSC). Figure 1 shows the TSC-TCR schematic diagram. I_Q is the total supply current.

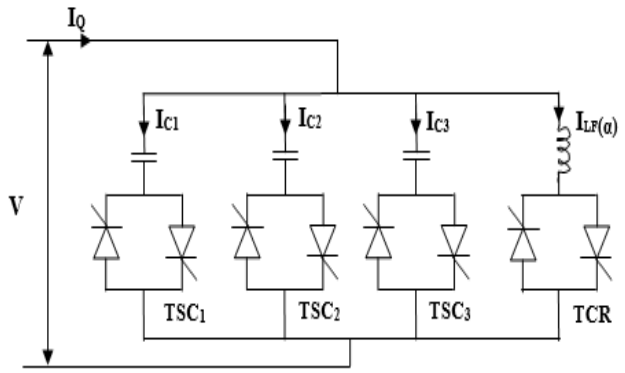

Figure 1: TSC-TCR schematic diagram (3TSCs, 1TCR)

The entire TSC-TCR scheme is operated in a closed loop manner in the sense that appropriate value of output signal Q is obtained as follows:

i. By determining the quantity of TSC branches that must be turned ON in order to roughly equal the required capacitive output current (with a positive surplus), as well as the amount of inductive current that must be cancelled out in order to eliminate the excess capacitive current.
ii. By control switching of the TSC branches in a transient-free manner.
iii. By varying the current in the TCR via firing delay angle control to cancel surplus Q demand of TSCs.

The net reactive power compensation is provided in a step-wise manner (continuous control) to boost power factor as reactive power demand increases.

The control scheme was implemented with a 3-phase circuit prototype for power factor control and improvement in a distributed laboratory environment. The basic equation models used are given as follows:

$$V = IR \quad (2)$$

Where, V is voltage measured in volts, I is current in amperes, R is resistance in ohms.

$$V_{rms} = \frac{V_{peak}}{\sqrt{2}} \quad (3)$$

$$I_{rms} = \frac{I_{peak}}{\sqrt{2}} \quad (4)$$

Where V_{rms} is rms voltage in volts, V_{peak} is maximum voltage in volts, I_{rms} is rms current measured in amperes, I_{peak} is maximum current in amperes. These were used to calibrate the voltage and current sensors.

To calculate for power factor control, the following equations were employed.

$$P = IV\cos\theta \quad (5)$$

Where P is real power in Watt

$$Q = IV\sin\theta \quad (6)$$

Where Q is the reactive power in VAR

$$\theta = 2\pi ft \quad (7)$$

Where θ is in radians or degrees, f is frequency in hertz, t is time in seconds

The key is to measure the angle between voltage and current (power factor angle, θ) and compensate the circuit with capacitor (TSCs) banks or inductor (TCRs) banks under different loading scenarios using phase switching control technique. An Arduino microcontroller (ATMEGA 2560) was programmed to use the phase control technique to monitor and bring in the capacitor and inductor banks while monitoring the overall power factor of the entire system under different loading conditions. Under these conditions, the microcontroller scanned and sampled the voltage and current waveforms, calculated the phase difference with the aid of voltage and current comparators and logic gate, converted the time duration between sample scans of voltage and current to phase angle and calculated the power factor. This circuit prototype was realized on a distributed level to demonstrate the behavior of a typical SVC in a laboratory environment.

2.2 Laboratory Implementation of TSC-TCR SVC Prototype

A low-cost microcontroller – based distributed SVC laboratory device was designed in Proteus software that has a controlled inductor (TCR) to adjust the power factor for load displacement in addition to switched capacitor banks (TSCs). This design was used to control the inductor and the capacitor banks for load power factor correction. There are three key implementation areas that were separately done and coupled together in the laboratory environment to meet the key objectives of this work which are: Implementation of Isolated Power logic supply, Implementation of Voltage/Current sensor section and Implementation of Microcontroller control of TSC-TCR.

2.2.1 Implementation of isolated power logic supply

The logic supply represented in Figure 2 was based on Transformer, Oscillator-driver circuit, switches, High frequency transformers, output switches (fast recovery/switching rectifiers) that led to the output. 240V ac was applied to the input and the transformer TR1 stepped it down to 2×15V ac. The transformer was an iron core type with center tap at the low voltage side operating at the frequency of 50Hz. A fuse rated 250V, 5A was added at the 240V side for protection and a switch to turn the circuit on and off. The secondary voltage was rectified by the diodes in full bridge configuration and the ac ripples were filtered by the paralleled electrolytic and ceramic (C1 50V, 2200µF and C2 520nF) capacitors. The dc voltage was fed into a flyback isolated dc-to-dc converter circuit which had four isolated outputs – two positive outputs and two negative outputs. This circuit was a half-bridge configuration making use of two capacitors C6 and C7, two metal oxide semi-conductor field effect transistors MOSFET, Q1 and Q2 and ferrite core transformers TR2 and TR3 for its operation.

A MOSFET driver (IRF740 signal generator) integrated circuit U1 drove the half-bridge MOSFETs at a frequency of 63kHz. U1 was biased with resistors R1 and R2, capacitors C3, C4 and C5 and a diode D2. The resistor R3 and R4 are the MOSFETs gate current limiting resistors while R5 and R6 are the pull-down resistors that ensure the MOSFETs gates reaches ground when turned off. The half-bridge circuit converted the dc output at C2 to high frequency ac which was applied to the transformers TR2 and TR3. The high frequency transformers had one primary and two secondary windings each. The induced voltages at the secondary windings were rectified back to dc voltages using fast switching diodes (FR207 rated 2A each), in full-bridge configurations. C9 – C14 are electrolytic and ceramic capacitors used to filter out ripples and the regulators U2 – U5 were used to maintain the voltage at fixed value (stiffened dc). LM7812 was used to regulate the positive voltages while LM7912 regulated the negative voltages.

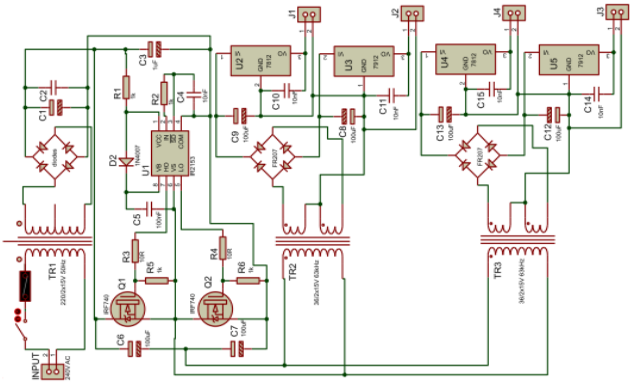

Figure 2: Circuit diagram of the logic supply

2.2.2 Implementation of voltage/current sensing section

This section is made up of the Signal conditioning (voltage waveform sensing, current sensing, exclusive OR gate (4070) and some parts of the microcontroller circuit (ATMEGA2560). The circuit schematic diagram is shown in Figure 3.

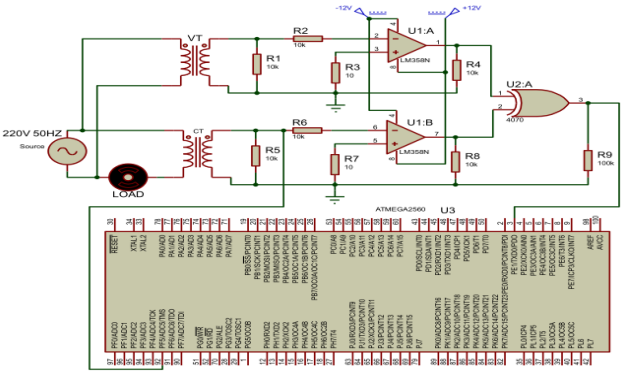

Figure 3: Schematic diagram of power factor measurement showing voltage and current sensing

A. Voltage sensing circuit

This comprises of a quad op amp comparator, U1A that was biased to compare the positive and negative signal waveform to zero changing them to square wave. Here, there is a voltage step-down transformer (220/6V) and a voltage divider circuit which was used to further divide the 6V by means of R1 and R2 resistors of 10kΩ each. The limiting resistor, R2 was sent to the inverting input of the op-amp while the non-inverting input was sent to ground through a low-resistance resistor R3 (10 Ω). The op-amp changed the sine wave to square wave. The op-amp which was configured in comparator mode with one leg on the ground through R3 should swing to lower voltage when the voltage of the second leg is zero. The op-amp receives 2 voltages (+12V/-12V) such that when the input is above zero, the output of the op-amp will be +12V. When the input is zero or below, the voltage will swing and give -12V output. R3 will be visible when there is output and zero (ground) when there is no output. Two voltage sensors were used to sense the voltage waveforms and rms voltage values.

B. Current sensing circuit

This compared the voltage waveform to a reference (zero) to change the sinusoid and generate a square wave. The Current transformer, CT that was used induced magnetic flux on the secondary coil creating a potential and the resistor R5 allowed the waveform to be viewed on the scope. From datasheet, the ratings of the CT are as follows: turns ratio 1:2000, 6V, range of resistance is 100-360Ω. This informed on the choice of resistors R5 and R6 which are 220Ω and

22Ω respectively. Also, when the CT allowed 10A to flow through the primary coil, a current of 5mA was induced in the secondary coil. Therefore, from ohms law:

$$5mA\ x\ 220\Omega = 1.1V \quad (8)$$

This was the voltage amplitude that the microcontroller sampled and converted to current and displayed. The current sensing circuit also had a quad op amp comparator, U1B biased to compare the positive and negative signal waveform to zero changing them to current square waveform.

C. The exclusive OR gate *(XOR- U2:A)*

This was rated at 3V-15V and used to capture the angular-phase displacement of the square waveforms for voltage and current. The displacement was utilized to compute the power factor and the resulting signal was sent to the microcontroller. By comparing two input bits, the XOR produces one output bit. According to the logic, if two bits are identical, the outcome is 0, and if two bits are different, the outcome is 1. Bits are generated via the XOR logic operation to provide fault tolerance and error checking. The phase angle was generated on the scope under purely resistive and inductive load conditions for the 3-phases. There are shown on the results section. The resistive load was a 200W bulb and the inductive load was a 3-phase, 3 h.p. AC machine (Induction motor).

2.2.3 Implementation of microcontroller (U3) control of TSC-TCR

The Microcontroller module, ATMEGA2560 -U3, has a total of 100 pins and operates at a maximum voltage of 5V. In this section, the microcontroller calculated the time and translated it to angle/degree using Equation 7. If it gets a high (1) as input from the XOR, it starts a timer until the output goes low and the timer stops. The time duration was used in calculating the angular difference between voltage and current and hence, the power factor was easily computed. The U3 took samples over a period of 20ms at the normal frequency of 50Hz. In other words, it took 20ms for the U3 to complete a full cycle of 360 degrees or 10ms for a half-cycle of 180 degrees. The U3 has a maximum voltage of 5V, so the Ardiuno was programmed to sample for 20ms and evaluate the sample points to get the peak value and continue to sample new values if the load was changed. The sampling process converted the analogue input signal to binary coded decimal value (BCD digitized value). Since the U3 can read a maximum of 5V, this implied that 1023 bytes was equivalent to 5V. This means that it sampled the 5V up to 1024 times (0 – 1023, 10-bit resolution). This was used to convert the BCD value to actual or real voltage. This voltage was the actual peak voltage divided by 1.4142 and multiplied by 1000.

Taking 9 sample points for instance, the actual peak voltage was calculated thus:

$$V_{peak} = \frac{5}{1023}\ x\ 9\ peak.sample.values.x\ 1000 = 43mV \quad (9)$$

Since the CT was biased with 220Ω, the Peak Current is,

$$I_{peak} = \frac{43mV}{220} = 0.000195A = peak\ values\ of\ current \quad (10)$$

$$\frac{I_{peak}}{\sqrt{2}}\ x\ 2000 = 0.28mA = actual\ value\ of\ current \quad (11)$$

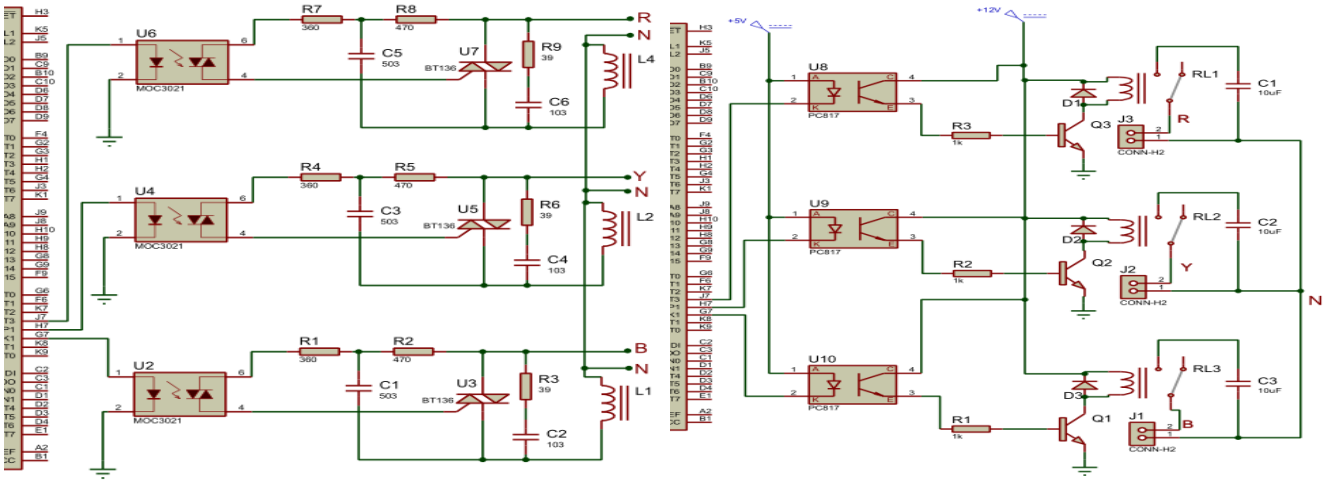

Figure 4: Capacitor (TSC) and inductive reactor switches (TCR) with microcontroller control

The positive half of the current/voltage waveform was sent to the U3. The U3 scanned and generated the rms values of each sample scan (summing and dividing by number of samples). The rms value was calibrated using a standard meter to measure the voltage and current values. Whatever the U3 interpreted the waveforms as in the form of a value, it was used to divide the measured voltage and current values to get

a ratio. This ratio became the conversion or correction factor that was used to multiply what the controller was giving as output (sensed output). Therefore, the correction/conversion factor was added to the program code for the microcontroller U3. This was how the rms values for voltage and current on all phases were calibrated. The Schematic diagrams of inductive reactor/Capacitor bank switch and control circuit are shown in Figure 4.

The Inductive reactors used an optocoupler and a TRIAC based on a semiconductor switch. The capacitor banks were configured with mechanically switched relays that solved a problem of "ringing effect" on the capacitor banks and heating of other components. The Optocoupler driver (MOC3021) comprised of an infrared LED and a photosensitive TRIAC switch. The optocoupler has a link to the microcontroller to know when to turn ON the switch. When d.c passed through the LED, it came ON and emitted light that switched on the Phototriac (hence there is no electrical connection). When the signal was non-zero, the LED was ON and OFF at zero. So, one side was connected to 5Vdc and the other to the Microcontroller unit. When the LED was OFF, the TRIAC was OFF and the microcontroller was seeing the 5V.

When the LED was ON (non-zero signal), the TRIAC was ON and drove the optocoupler and the microcontroller to ground. In other words, anytime the microcontroller saw 5V, it will know that the optocoupler is on ground level (OFF) and the signal is crossing zero. While at any other time the signal is not crossing zero, the microcontroller will be seeing zero. This is the "zero crossing circuit" principle. Fixed capacitors were not used for compensation because the microcontroller calculated to see the needed value of compensation by using the thyristor phase control technique of switching to make the effectiveness of the compensators in the network to match the needed compensation level. The resistors (R1-R8) around the TRIAC, BT136 formed a snubber circuit used to reduce gating current to the TRIAC gate. The Microcontroller controlled the compensators (Inductive reactors and Capacitor banks) through the optocoupler. These compensators were all connected to a 3-phase switch where 3-phase load could be connected. There was a 4-pin display screen that showed the output parameters of the implemented SVC.

3.0 RESULTS AND DISCUSSION

3.1 Implementation from the Results of the TSC-TCR

This section presented the transient and steady-state waveforms of phase voltage, line-current and line voltages with respect to the implemented TSC-TCR scheme under resistive and inductive loading conditions with the aid of RICOL and HANTEK-made oscilloscopes. Figure 5 presents the steady-state phase voltage waveforms for resistive loads.

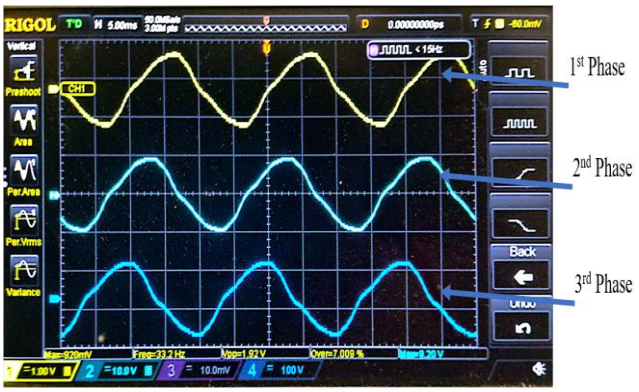

Figure 5: Steady-state phase-voltage under purely resistive loads (three - 200W bulbs)

Figure 6: Steady-state phase-voltage under purely inductive load (3-ϕ, 3-h.p induction motor)

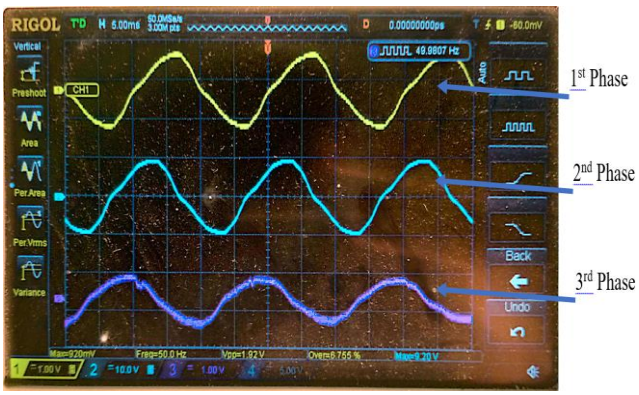

Figure 7: Transient phase-voltage under purely resistive loads (three - 200W bulbs)

From Figure 5, it can be seen that the waveforms were minimally distorted under this loading condition. The distortions were as a result of the three-200W bulbs which are resistive in nature. The waveforms are

displaced by 120^0. Figure 6 presents the steady-state phase voltage waveforms for inductive loads. It can be seen that the steady state waveforms were more distorted than the resistive load condition (of Figure 5) especially in the first two phases as a result of the practical efficiency of the three-phase, three h.p induction motor under test. This waveshape indicates that the motor drew more current than the resistive 200W bulbs. Figure 7 presents the transient phase voltage waveforms for resistive loads.

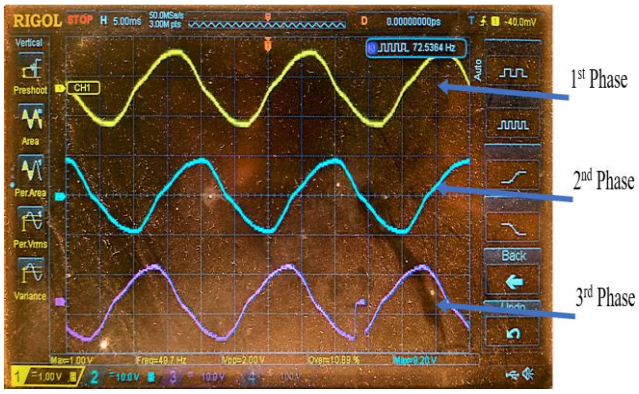

Figure 8: Transient phase-voltage under purely inductive loads (3h.p induction motor)

It is seen that the transient occurred at -4 seconds and -0.5 seconds respectively with minimal distortion in waveshape. This was as a result switching of the circuit components and addition of Load. Figure 8 presents the transient phase voltage waveforms for inductive loads. It is seen that the transient occurred at 3.5 seconds with more distortion in waveshape as a result of variations in stator and rotor currents of the motor due to switching. Figure 9 presents the steady-state line voltage waveforms for resistive loads.

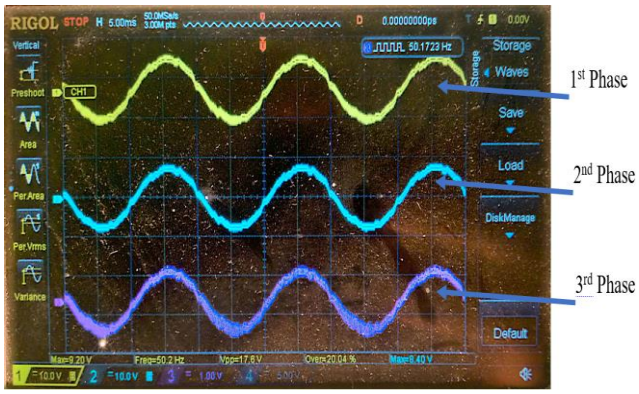

Figure 9: Steady state line voltages under same resistive loads (three - 200W bulbs)

It can be seen that the phase-to-phase voltage waveforms were bolder and continuous with minimum distortions due to the resistance of the bulbs. Figure 10 presents the steady-state line voltage waveforms for inductive loads. This scope showed more distortions in amplitude and waveshape happening at every period due to the inductive nature of the AC machine. Figure 11 presents the transient line voltage waveforms for resistive loads.

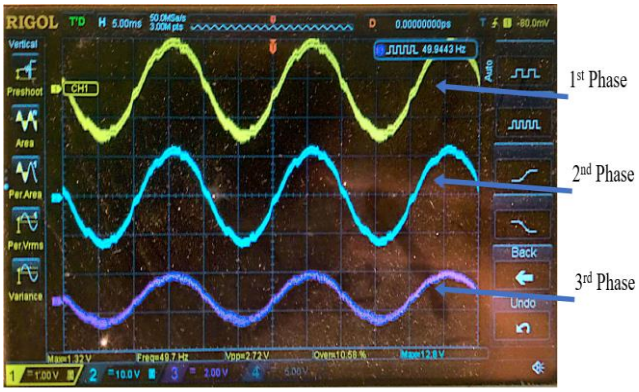

Figure 10: Steady state Line voltage under inductive loads (3h.p induction motor)

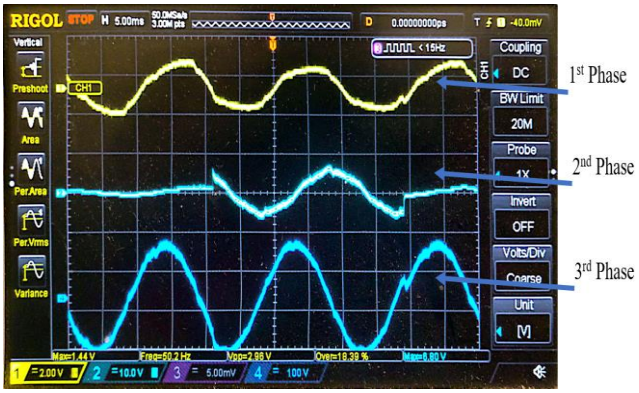

Figure 11: Transient line voltage under resistive loads (three - 200W bulbs)

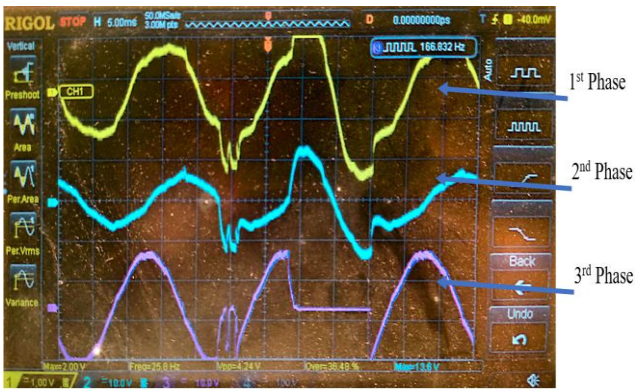

Figure 12: Transient line voltage under Inductive loads (3 hp Induction motor)

Figure 11 showed that the transients occurred at most points on the waveforms with more distortion on phase 2 with visible changes in amplitude. Figure 12 presents the transient line voltage waveforms for inductive loads. The transients occurred at -1s, 1s and 3 seconds with significant harmonic distortions on all

the phases due to the inductance of the AC machine (high starting current). Figure 13 presents the steady-state line current waveforms for resistive loads. From Figure 13, the line currents showed thicker waveforms with minimal distortions due to the effective resistance of the bulbs. Figure 14 presents the steady-state line current waveforms for inductive loads.

Figure 13: Steady state line current under resistive loads (three - 200W bulbs)

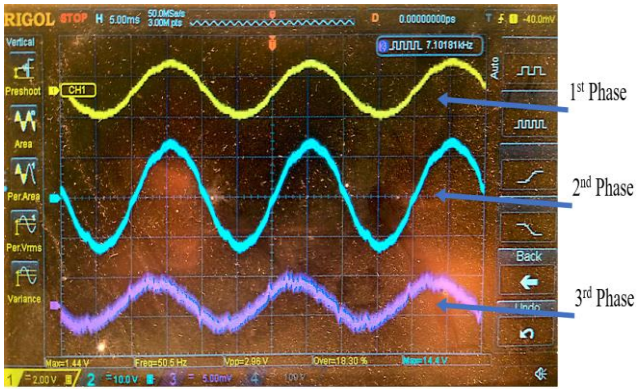

Figure 14: Steady state line current under inductive loads(3 hp Induction motor)

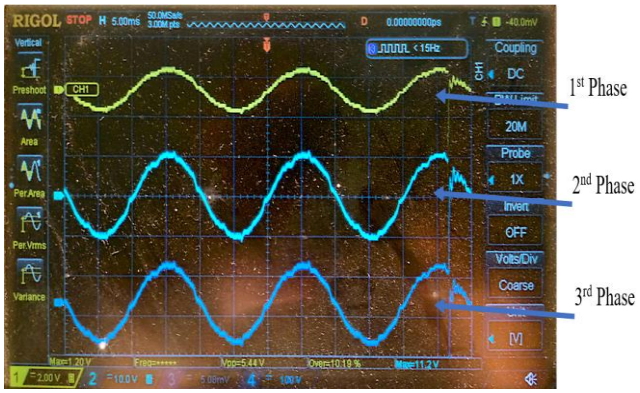

Figure 15: Transient line current under resistive loads (three - 200W bulbs)

From Figure 14, the induction motor under test gave line currents with thicker waveforms and more distortions in amplitude and waveshape. This is as a result of its design and performance characteristic nature. Figure 15 presents the transient line current waveforms for resistive loads.

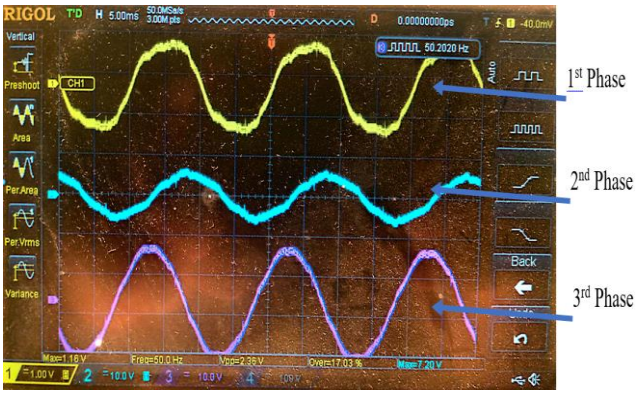

Figure 16: Transient line current under inductive loads(3 hp Induction motor)

Figure 15 showed that the transients occurred mostly at 5.5seconds on the three phases simultaneously. At this time, harmonics occurred across the three-phases as a 3-phase fault condition due to component switching. Figure 16 presents the transient line current waveforms for inductive loads.

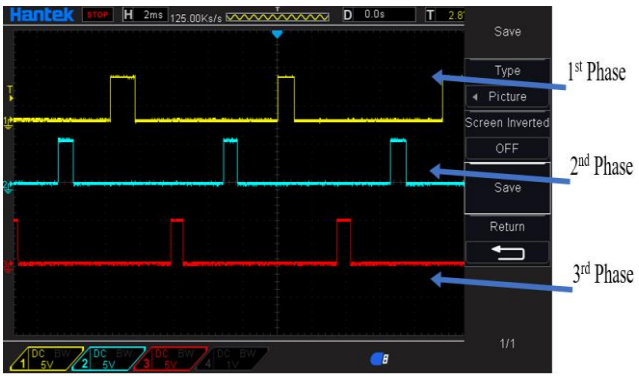

Figure 17: Phase difference with 200W x 3 purely resistive loads on the three phases

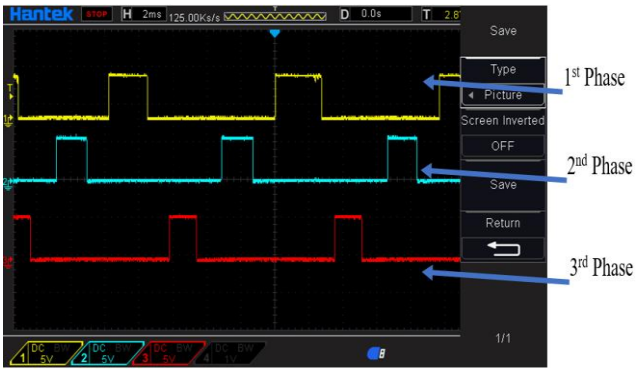

Figure 18: Phase difference with 3-phase, 3 h.p. AC Induction motor load

Figure 16 showed the transients occurring at many points with harmonic distortions of waveshape-amplitude due to AC machine inductance. Figure 17

shows the Voltage phase difference for purely resistive loads on the three phases. It is seen that there is minimum phase angle difference between the voltages and currents. Figure 18 shows the phase difference of the SVC under 3-phase inductive load.

This shows further increase in phase difference for the three phases due to inductive nature of AC motor. Figures 19 and 20 show a Liquid crystal display (LCD) that presents the overall output parameters of the implemented 3-phase SVC system at no-load and under load.

Figure 19: LCD display showing the display output parameters when the SVC is switched ON at no load

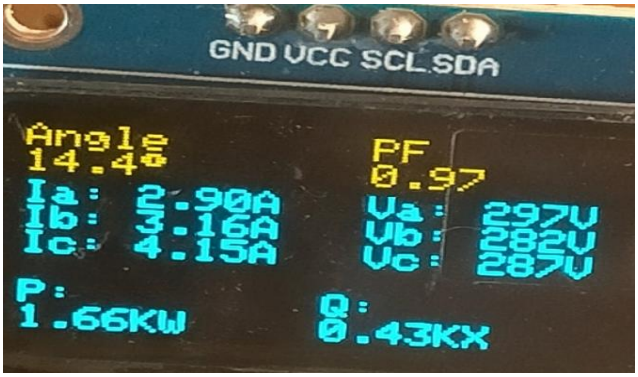

Figure 20: LCD display showing the display output parameters when the capacitor bank switches to compensate the load after 120 seconds

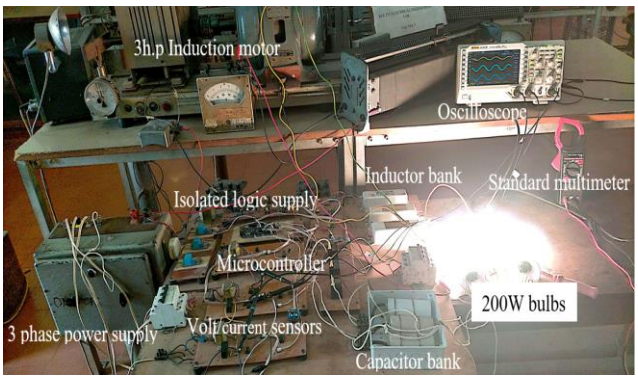

Figure 21: Complete Implemented TSC-TCR SVC circuit with all the sections

The power factor is at normal value of 0.98 and when the Inductive reactor loads initiate, the power factor comes down to 0.67 due to inductive loading. The power factor is restored back to 0.97 due to SVC action. Generally, it is observed from the LCD display that under inductive loading, the power factor increased significantly from 0.67 to 0.97 due to SVC action. The real power increased from 0.37kW to 1.66kW and the reactive power improved from 0.41kVAR to 0.43kVAR. The full laboratory implementation diagram is shown in Figure 21. The total cost for implementing this work was ₦ 99,099 which is economically viable.

4.0 CONCLUSION

The ever-growing demand for power because of the population growth in developing countries has raised demand for implementation of FACTS devices to optimize their power systems. The microcontroller-based TSC-TCR SVC prototype was implemented in a laboratory environment that automatically calculated and improved the power factor significantly from 0.67 to 0.97 (44.78% increase) under inductive loads. This study helps us to understand that a basic FACTS device can be realized with locally available materials which is economical in Nigeria and other less-developed countries.

5.0 ACKNOWLEDGEMENTS

The Department of Electrical Engineering, University of Nigeria, Nsukka, Nigeria, and the management of Laboratory of Industrial Electronics, Power Devices and New Energy Systems (LIEPNES) are acknowledged and appreciated by the authors for providing a favourable place to implement this study.

6.0 CONFLICT OF INTEREST

The authors hereby affirm that they have no conflict of interest regarding this research to declare.

REFERENCES

[1] Olanipekun, B. A., Adelakun, N. O., and Okoye, C. U. “Evaluation of Electrical Services using Energy Efficient Load”, *Journal of Scientific and Engineering Research*,” vol. 7, no. 2, pp. 165-170, 2020.

[2] Airoboman, A. E., John, S. N., Araga, I. A., Abba-Aliyu, S., and Aderibigbe, M. A. "Power-Flow Analysis of Shiroro-Jebba-Oshogbo 330-kV Transmission Network Cluster", *2021 IEEE PES/IAS PowerAfrica*, Nairobi, Kenya, 2021, pp. 1-5.

[3] Badrudeen, T. U., Ariyo, F. K., Gbadamosi, S. L., and Nwulu, N. I. “A Novel Classification of the 330 kV Nigerian Power Network Using a

New Voltage Stability Pointer", *Energies*, vol. 15, no. 19, 2022.

[4] Buraimoh, E., Ariyo, F. K., Omoigui, M. O., and Davidson I. "Investigation of Combined SVC and TCSC versus IPFC in Enhancing Power System Static Security", *International Journal of Engineering Research in Africa, JERA*, vol. 40, pp. 119–135, 2018.

[5] Okechukwu U. K., and Onoh, G. N. "Loss Minimization of the Nigeria 330kV Power Grid Network Using Artificial Neural Network Based Interline Power Flow Compensator", *European Journal of Engineering and Environmental Sciences*, vol. 6, no. 5, pp. 1-13, 2022.

[6] Braide, S. L. "Evaluation and Analysis of Harmonic Distortion on 330kV Network Case Study Selected Sub-Region Nigerian Power System for Improve Power Quality", *Journal of progress in engineering and physical science*, vol. 1, no. 1, 13–2, 2022.

[7] Ezeruigbo, E. N., Ekwue, A. O., and Anih, L. U. "Voltage Stability Analysis of Nigerian 330kV Power Grid using Static P-V Plots", *Nigerian Journal of Technology, NIJOTECH*, vol 40 no.1, 2021.

[8] Amole, A. O., Oladipo, S., Olabode, O. E., Makinde, K. A., and Gbadega, P. "Analysis of grid/solar photovoltaic power generation for improved village energy supply: A case of Ikose in Oyo State Nigeria", *Renewable Energy Focus*, vol. 44, pp. 186-211, 2023.

[9] NERC reports "Generation", https://nerc.gov. ng/index.php/home/nesi/403-generation, Accessed on June 10, 2021.

[10] Umunnakwe, A., Alimi, A., Davis, K. R., and Butler-Purry, K. L. "Improving Situational Awareness in Power Grids of Developing Countries: A Case Study of the Nigerian Grid", *2023 IEEE Power & Energy Society Innovative Smart Grid Technologies Conference (ISGT)*, Washington, DC, USA, 2023, pp. 1-5.

[11] Olukan, T. A., Santos, S., Al Ghaferi, A. A., and Chiesa, M. "Development of a solar nano-grid for meeting the electricity supply shortage in developing countries (Nigeria as a case study)", *Renewable Energy*, vol. 181, pp. 640-652, 2022.

[12] Osman, M., Taylor, G., Rawn, B., and Nwachukwu, T. "Development of Excitation System Modelling Approaches for the Nigerian Grid", *2021 56th International Universities Power Engineering Conference (UPEC)*, Middlesbrough, United Kingdom, 2021, pp. 1-5.

[13] Ogar, V. N., Gamage K. A. A., and Hussain. S. "Protection for 330 kV transmission line and recommendation for Nigerian transmission system: a review", *International Journal of Electrical and Computer Engineering*, vol. 12, no. 3, pp. 3320-3334, 2022.

[14] Ogar, V. N. "Modelling of a protective scheme for AC 330 kV transmission line in Nigeria", *PhD dissertation*, University of Glasgow, 2023.

[15] Abdulkareem, A., Adesanya, A., Agbetuyi A. F., and Alayande, A. S. "Novel approach to determine unbalanced current circuit on Nigerian 330kV transmission grid for reliability and security enhancement", *Celpress Journal, Heliyon 7*, 2021.

[16] Onah, C. O., Agber, J. U., and Inaku, I. O. "The Impact of Static Synchronous Compensator (STATCOM) on Power System Performance: A Case Study of the Nigeria 330kV Power System Network", *The International Journal of Engineering and Science (IJES)* vol. 9 no. 7, pp. 42-52, 2020.

[17] Ahiakwo, C. O., Idoniboyeobu, D. C., Braide, S. L., and Onita, C. L. "Investigation of Voltage Stability of the Nigerian 330kV Transmission Network Using Newton Raphson Method", *International Journal of Research in Engineering and Science (IJRES)*, vol.10, no. 6, pp. 122-129, 2022.

[18] Okechukwu U. K., and Onoh, G. N. "Characterization and Development of a Simulink Model of 330kV Nigeria Power Transmission Network", *American Journal of Applied Sciences and Engineering*, vol. 3, no. 6, pp 38-50, 2022.

[19] Abdulkareem, A., Somefun, T. E., Awosope, C. O. A., and Olabenjo, O. "Power system analysis and integration of the proposed Nigerian 750-kV power line to the grid reliability", *Springer Nature Applied Sciences*, vol. 3, no. 864, 2021.

[20] Nnoli, K. P., Kettemann, S., Benyeogor M. S., and Olakanmi, O. O. "A Dynamic Model of Realistic Nigerian 330 kV Transmission Network: A Catalyst to Realistic Grid Studies and Expansion Strategy", *2021 International Conference on Electrical, Computer and Energy Technologies (ICECET)*, Cape Town, South Africa, 2021, pp. 1-9.

[21] Ukiwe, E. K., Adeshina S. A., and Jacob, T. "Evaluating Effects of Power Sector Regulation on System Stability during Optimal Operation of Nigeria's 330kV Power Grid", *2021 1st International Conference on Multidisciplinary*

Engineering and Applied Science (ICMEAS), Abuja, Nigeria, 2021, pp. 1-6.

[22] Olasunkanmi, O. G., Deng Z., and Todeschini, G. "Load Flow Analysis of the Nigerian Transmission Grid Using DIgSILENT PowerFactory", *2021 56th International Universities Power Engineering Conference (UPEC)*, Middlesbrough, United Kingdom, 2021, pp. 1-6.

[23] Narain, A., and Srivastava, S. K. "An Overview of Facts Devices used for Reactive Power Compensation Techniques", *power*, vol. 2, no. 12, p. 3, 2015.

[24] Ikonwa, W., Obuah, E. C., and Wokoma, B. "Impact of Static Var Compensator (SVC) on Transient Stability of Power Network in Nigeria", *International Research Journal of Innovations in Engineering and Technology (IRJIET)*, vol. 7, no. 4, pp. 37-44, 2023.

[25] Nkan, I., Obi, P., Natala, H., and Okoro, O. "Investigation of the Transfer Capability of the Nigerian 330 kV, 58-bus Power System Network using FACTS Devices", *ELEKTRIKA- Journal of Electrical Engineering*, vol. 22, no. 1, 2023, pp. 53–62.

[26] Nkan, I. E., Okpo, E. E., and Okoro, O. I. "Multi-Type FACTS Controllers for Power System Compensation: A Case Study of the Nigerian 48-Bus, 330kV System", *Nigerian Journal of Technological Development*, vol. 18 no. 1, 2021, pp. 63-69.